Received: 6 October 2018 | Revised: 21 March 2019 | Accepted: 22 March 2019

DOI: 10.1002/aoc.4951

FULL PAPER

WILEY Applied Organometallic Chemistry

A convenient room temperature *ipso*-nitration of arylboronic acid catalysed by molecular iodine using zirconium oxynitrate as nitrating species: An experimental and theoretical investigation

Abhijit Mahanta[1] | Nanda Kishor Gour[1] | Plaban Jyoti Sarma[1] | Raju Kumar Borah[1] | Prasanta Kumar Raul[2] | Ramesh Chandra Deka[1] | Ashim Jyoti Thakur[1] | Utpal Bora[1]

[1]Tezpur Central University, Tezpur (Napaam), Assam 784028, India

[2]Defence Research Laboratory, Tezpur, Assam 784001, India

Correspondence
Ashim Jyoti Thakur and Utpal Bora, Tezpur Central University, Tezpur (Napaam), Assam, 784028, India.
Email: ashim@tezu.ernet.in; utbora@yahoo.co.in

Funding information
Tezpur University; DST-SERB, Grant/Award Number: EMR/2016/005944

A simple and convenient protocol has been developed for *ipso*-nitration of arylboronic acid catalysed by molecular iodine at room temperature, using zirconium oxynitrate as the nitrating species. The protocol is applicable to electronically diverse aryl- and heteroarylboronic acid moieties under mild reaction conditions with good to excellent isolated yields. Furthermore, a theoretical investigation has been performed for the same reaction, and reaction profiles are modelled using modern density functional theory (DFT). DFT-based results support the experimentally observed results.

KEYWORDS
iodine, *ipso*-nitration, zirconium oxynitrate

1 | INTRODUCTION

In the challenging domain of synthetic organic chemistry, nitration of arenes has emerged as one of the most fundamental and important organic transformation reactions, both for academic interest and industrial applications. In real terms, over the decades, nitroarenes have shown their potentialities by contributing to varieties of important areas like pharmaceuticals, dyes and plastics.[1–4] They have also been used as explosives and precursors for azo dyes.[5] This indispensable significance in organic synthesis may be attributed to their easy availability, ease of transformation to other functional groups and the ability of nitroaryl moieties to impart tunable physical and chemical properties to many structurally targeted organic molecules. In general, the traditional method for synthesis of nitroarenes involves electrophilic nitration of arenes in the presence of excess amount of conc. sulfuric acid and nitric acid under harsh reaction conditions which are problematic, primarily due to the involvement of strong acid and secondly to the requirement of high temperature. Another common reagent for nitration of arenes is dinitrogen pentoxide, which is a hazardous oxidizer and an important reservoir[6,7] for NOx that are responsible for ozone layer depletion and acid rain. Additionally, regioselectivity is a major issue in traditional methods as the reaction is often associated with other oxidation products and mixtures of isomers.[8] Therefore, looking for some efficient alternative strategies eliminating the drawbacks of existing methodologies has significance which has attracted considerable attention among researchers and has become a long-standing challenge for synthetic organic chemists. In contemporary organic synthesis, as far as nitration of arenes is concerned, *ipso*-nitration occupies a much superior position. In 2009, Fors and Buchwald reported[9] the nitration of aryl chlorides, triflates and nonaflates to nitroaromatics catalysed by Pd. It is a fascinating protocol, but use of expensive ligand-based Pd catalyst limits its practical application. An efficient Cu-catalysed protocol for the

conversion of aryl iodides to nitrobenzene was reported by Saito and co-workers.[10] There are other reported methodologies that include nickel nitrate-catalysed nitration of phenolic compounds,[11] microwave-assisted formation of nitrorenens from phenolic compounds,[12] etc.

Aryl halides and phenolic compounds are known environmental pollutants.[13] Additionally, by-products of aryl halides invite problems during isolation and purification of desired products. In this context, nowadays, arylboronic acids have emerged as interesting and versatile alternative organic synthons for this type of transformation as they offer some significant and preferable properties such as non-toxicity, heat and moisture resistance and easy availability with varying substitutions.[14] Some reagents/catalysts have been reported for the transformation of arylboronic acids to nitroarenes, e.g. $Bi(NO_3)_3$/$K_2S_2O_8$,[15] TMS-Cl/MNO_3[16] (M = Ag, NH_4), Cu_2O/$NaNO_2$,[17] etc. Catalyst-free conversion of arylboronic acids to nitrobenzenes has also been carried out with bismuth nitrate[18] and iron nitrate[19] as nitrate sources. Additionally, *ipso*-nitration has been carried out with *tert*-butyl nitrite[20] as the nitrate source under catalyst-free conditions (Scheme 1).

Although some reports claim successful *ipso*-nitration of arylboronic acids, yet, in most cases, use of strong acids,[21] prolonged reaction time (30–72 h), high temperature,[22] etc., were necessary to maximize catalytic performances. Moreover, many of them suffer limitations regarding poor substrate scope and intolerance to heterocyclic moieties. Therefore, a highly active catalytic system is still desired for the said reaction protocol, which avoids the drawbacks like using high temperature, strong acid, etc., because these drawbacks go against the 'green sustainable chemistry' principles.

Taking into consideration the points mentioned above, herein, we report a facile and practical method for *ipso*-nitration of arylboronic acids in the presence of molecular iodine (I_2) as catalyst, zirconium nitrate as nitrating source and toluene as solvent. In recent times, there has been an increasing interest in molecular iodine-catalysed organic transformations owing to its numerous advantages such as it being a powerful, inexpensive, non-toxic and readily available catalyst.[23] This has also relevance

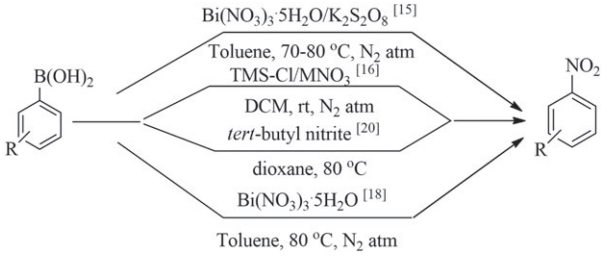

SCHEME 1 Previous works on *ipso*-nitration reaction

with regard to green chemistry. Also, easily available $ZrO(NO_3)_2{\cdot}XH_2O$ is a safe and easy-to-handle nitrating source.[24] In order to provide strong support to the experimental work for the reaction under investigation, theoretical calculations were performed using density functional theory (DFT). Here, based on these findings, we present feasibility of the reaction and exploration of the reaction pathway on potential energy surface (PES) along with transition state (TS). Intrinsic reaction coordinate (IRC) calculation was also performed to confirm the smooth transition from reactant to product through the respective TS.

To optimize our *ipso*-nitration protocol, we planned to investigate the reaction with different nitrate sources such as cupric nitrate, ammonium nitrate, cobalt nitrate, silver nitrate, zirconium oxynitrate, etc. To begin with, a round-bottomed flask was charged with 1 mmol of phenylboronic acid as the model substrate and cupric nitrate (2 mmol) as the nitrating agent under stirring followed by heating to 80°C. Initially, we decided to perform the reaction with 15 mg of montmorillonite (K10) clay as an acidic additive and it showed very little conversion to nitroarenes along with formation of phenol as the side product (Table 1, entry 1). Interestingly, the reaction without K10 showed no conversion to nitroarene at all. This particular result signified the importance of acidic additive for targeted nitrobenzene product.

For the next assessment, we carried out the reaction with diverse nitrate salts. When we replaced the cupric nitrate salt by ammonium nitrate, cobalt nitrate, silver nitrate and sodium nitrate, formation of phenol discontinued but the yield of the nitroarene was found to be moderate (Table 1, entries 2–5). However, we observed slightly better results with zirconium oxynitrate salt as nitrating source (Table 1, entry 6). Further, fixing $ZrO(NO_3)_2{\cdot}XH_2O$ (2 mmol), oxidants were altered with the aim of achieving better conversion. Progress of the reaction was checked with solid acids such as *p*-toluenesulfonic acid (*p*-TSA), silica, alumina, etc. However, no noticeable improvement in result was observed (Table 1, entries 7–9). Interestingly, use of *o*-phosphoric acid as an oxidant gave better conversion with $ZrO(NO_3)_2{\cdot}XH_2O$ as the nitrate source (Table 1, entry 10). However, acetic acid as an acid failed to afford a good conversion of the desired product nitrobenzene. Interestingly, the reaction catalysed by molecular iodine showed the best conversion with trace amount of nitrosobenzene (Table 1, entry 12) in 12 h at 80°C. Moreover, when using other additives such as silica or K10 along with molecular iodine, the reaction completed quickly although formation of nitrosobenzene was also observed. Then, we proceeded to investigate the reaction with iodine (20 mol%) as oxidant and tried with other nitrate sources

TABLE 1 Optimization of reaction conditions[a] for different additives, nitrate salt, amount of catalyst and temperature

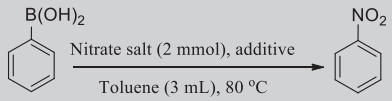

Entry	Nitrate salt	Additive	Time (h)	Yield (%)[b]
1	Cupric nitrate	K10 (15 mg)	24	20
2	Ammonium nitrate	K10 (15 mg)	24	25
3	Cobalt nitrate	K10 (15 mg)	24	40
4	Silver nitrate	K10 (15 mg)	24	8
5	Sodium nitrate	K10 (15 mg)	24	13
6	Zirconium oxynitrate	K10 (15 mg)	24	55 + 5% nitroso
7	Zirconium oxynitrate	*p*-TSA (15 mg)	24	42
8	Zirconium oxynitrate	Silica (15 mg)	24	34 + 15% nitroso
9	Zirconium oxynitrate	Alumina (15 mg)	24	45
10	Zirconium oxynitrate	H_3PO_4 (2 ml)	24	84
11	Zirconium oxynitrate	CH_3COOH (2 ml)	24	23
12	Zirconium oxynitrate	I_2 (20 mol%)	12	89 + 5% nitroso
13	Cupric nitrate	I_2 (20 mol%)	12	45
14	Cobalt nitrate	I_2 (20 mol%)	12	25
15	Ammonium nitrate	I_2 (20 mol%)	12	20
16	Silver nitrate	I_2 (20 mol%)	12	28
17	Sodium nitrite	I_2 (20 mol%)	12	30
18	Zirconium oxynitrate	I_2 (15 mol%)	12	89
19	Zirconium oxynitrate	I_2 (10 mol%)	12	89
20	Zirconium oxynitrate	I_2 (5 mol%)	24	67
21[c]	Zirconium oxynitrate	I_2 (10 mol%)	18	89
22[c,d]	Zirconium oxynitrate	I_2 (10 mol%)	18	89
23[c,e]	Zirconium oxynitrate	I_2 (10 mol%)	18	65
24[c,d,f]	Zirconium oxynitrate	I_2 (10 mol%)	12	92

[a]Reaction conditions: phenylboronic acid (1 mmol), nitrate salt (2 mmol), toluene (3 ml).

[b]Isolated yield.

[c]Room temperature *ca* 34°C in air, unless otherwise noted.

[d]1.5 mmol of the nitrate salt was used.

[e]1 mmol of the nitrate salt was used.

[f]Under nitrogen atmosphere.

(Table 1, entries 13–17). Again, we found zirconium nitrate as the most suitable nitrating agent for the *ipso*-nitration protocol.

Several test reactions were carried out using different amounts of I_2 to optimize the amount of catalyst for maximum yield of product. It has been observed that with 20 mol% of the catalyst (molecular iodine), the reaction completed in 12 h (Table 1, entry 12). Then, the reaction was carried out with 15, 10 and 5 mol% (Table 1, entries 18–20) of catalyst under the same reaction conditions. Comparable yield was obtained with 15 and 10 mol% of the catalyst in 12 h. However, the reaction with 5 mol% of the catalyst did not show completion even after 24 h. Interestingly, when the reaction was carried out at room temperature using 10 mol% of the catalyst, to our delight, the reaction completed with the same yield of conversion in 18 h (Table 1, entry 21). Later, by varying the amount of the nitrate salt, we found the best result with 1.5 mmol of the nitrate salt (Table 1, entry 22), and further reducing the amount nitrate salt to 1 mmol afforded lower yield of the product (Table 1, entry 23). To investigate the effect of air in the reaction, we performed a reaction under

TABLE 2 Molecular iodine-catalysed synthesis of nitrobenzene from arylboronic acids[a]

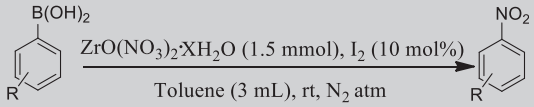

Entry	R	Time (h)	Yield (%)[b,c]
1	H	12	89
2	4-Bromo	18	84
3	4-Formyl	12	85
4	3-Formyl	20	79
5	2,4-Dichloro	18	85
6	3-Chloro	18	87
7	4-Hydroxy	16	85
8	4-Amino	12	89
9	4-Methoxy	12	86
10	2-Methyl	20	78
11	4-Methyl	16	81
12	2-Thiophenyl	8	83
13	2-Methoxy-6-pyridyl	11	80
14	4-Fluoro	14	86
15	2,4-Difluoro	17	86
16	2-Chloro	16	84
17	4-Chloro	14	88

[a]Reaction conditions: phenylboronic acid (1 mmol), nitrate salt (1.5 mmol), toluene (3 ml).

[b]Isolated yield.

[c]Under nitrogen atmosphere.

nitrogen atmosphere keeping all other reaction parameters the same as in entry 24 of Table 1. Interestingly, we observed a better result with exclusive formation of nitrobenzene. Formation of by-product nitrosobenzene was completely eliminated under nitrogen atmosphere. Additionally, the reaction completed within a short time interval in comparison to air atmosphere. To study the effect of solvents in our system, the reaction was investigated with various polar, non-polar, protic and aprotic solvents. Among the aprotic solvents such as toluene, xylene, dichloromethane (DCM) and chloroform, except toluene and xylene, the others failed to show efficiency as good solvents. The reaction did not proceed smoothly in dimethylsulfoxide, isopropanol, methanol and water and showed poor conversion. Between toluene and xylene, we consider toluene as the best solvent.

With the optimized reaction conditions (Table 1, entry 24), further study of the generality of the *ipso*-nitration protocol was extended to a variety of substituted arylboronic acids (Table 2, entries 1–17). Phenylboronic acids having electron-withdrawing as well as electron-donating groups were also found to give corresponding nitrobenzene in excellent yields. Heteroarylboronic acids provided moderate results (Table 2, entries 12 and 13). Interestingly, no significant effects were observed for sterically demanding arylboronic acid moieties (Table 2, entries 5, 10, 12, 13, 15 and 16) as well as electron-donating and electron-withdrawing substrates.

It has been reported that the *ipso*-nitration of arylboronic acids usually progresses through a free radical pathway.[19] So, to investigate the reaction mechanism, at first we performed a radical trapping experiment by using stoichiometric amount of radical scavenger 2,2,6,6-tetramethylpiperidine-*N*-oxide (TEMPO). We added TEMPO to the reaction mixture under the same conditions but the reaction was found to progress even after addition of the same; this result ruled out the possibility of a radical mechanism for the current reaction protocol.

Therefore, we have suggested a plausible mechanistic pathway based on the reported non-radical pathway,[16] as shown in Figure 1. It is believed that, initially, iodine (I_2) molecule reacts with nitrate salt [$ZrO(NO_3)_2H_2O$] to form $IONO_2$ and $ZrO(NO_3)(H_2O)I$ species. Subsequently the oxygen atom of $IONO_2$ species reacts at electron-deficient boron atom of arylboronic acid via the lone pair of electrons and forms an intermediate (A) which rearranges to form the desired nitrobenzene product and $IOB(OH)_2$ species. It is also important to note that the by-products of step 1 [$ZrO(NO_3)(H_2O)I$] and step 2 [$IOB(OH)_2$] combine with each other to form $ZrO(NO_3)(OH)$ complex and H_3BO_3 molecule and regeneration of I_2 as shown in step 3.

To visualize the reaction mechanism and thermochemistry of the main step (step 2) along with the other two steps as given in Figure 1, a theoretical investigation was performed using the DFT approach. Optimized structures of all species (including intermediates and TSs) involved in the title reaction (steps 1, 2 and 3) were obtained with B3LYP functional along with 6-311G+(d)/LanL2DZ basis sets as shown in Figure 2. In the first step, when I_2 reacts with [$ZrO(NO_3)_2(H_2O)$], a reaction complex (RC1) and TS (TS1) are formed before the formation of products. In RC1, we observed that the bond distances between Zr atom and two O atoms of [$ZrO(NO_3)_2(H_2O)$] are found to be 2.397 Å and 2.284 Å. These observed bond distances are longer than the Zr–O bond lengths (2.299 Å and 2.305 Å) in the parent [$ZrO(NO_3)_2(H_2O)$] complex. In addition, the distances of two I atoms of I_2 with Zr and O atoms of the complex are found to be 3.406 Å and 2.715 Å, while distance between I_2 is 3.397 Å. In TS1, Zr–O distances further increase from RC1 and became 2.414 Å and 2.379 Å, respectively. It is also found that bond distance of newly formed Zr–I and O–I bonds increased in TS1, which indicates the breaking of Zr–O

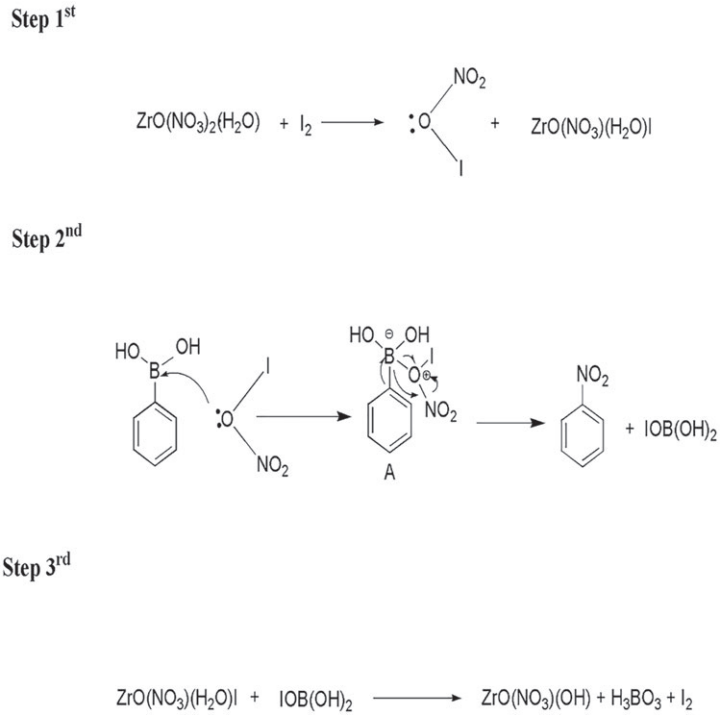

FIGURE 1 Reaction steps for the formation of nitrobenzene and I_2 regeneration

and I_2 bonds and formation of $IONO_2$and [$ZrO(NO_3)(H_2O)I$] species via product complex (PC1). In the next steps, $IONO_2$ reacts with arylboronic acid leading to the formation of RC2, then proceeding via TS2 to give the final product via PC2. In RC2, N and O atoms of $IONO_2$ are making bonds with the C and B atoms of arylboronic acid at distances of 2.978 Å and 2.267 Å, respectively. In TS2, the respective bond distances are decreased to 2.247 Å and 1.614 Å and reveal the formation of C–N and O–B bonds. Moreover, it was observed that the N–O distance in $IONO_2$ increases from 1.552 Å to 1.963 Å with respect to RC2. During the formation of products [nitrobenzene + $IOB(OH)_2$], C–B and N–O bonds break completely and C–N and O–B bonds are formed. In the last step, the by-products of previous steps react together to give RC3 which further regenerates I_2 via TS3 along with [$ZrO(NO_3)(OH)$] and H_3BO_3. In RC3, O–H and Zr–I distances are increased to 1.069 and 3.296 Å with respect to initial bond parameters of [$ZrO(NO_3)(H_2O)I$] and also O–I distance is increased to 2.216 Å from the initial $IOB(OH)_2$ species. In TS3, the bond distances of O–H and Zr–I increase to 1.350 Å and 3.351 Å compared to the distances in RC3. The O–I distance increases to 2.299 Å in TS3, while distance between I_2 decreased to 3.035 Å compared to that in RC3. Finally, O–H and Zr–I bonds break in [$ZrO(NO_3)(H_2O)I$] and O–I bond breaks in $IOB(OH)_2$ and forms O–H bond in $IOB(OH)_2$ and I_2 is completely regenerated.

Vibrational frequency calculations were further performed for all of the optimized structures involved in the various steps at same level of theory to understand the various modes of vibrations (real or imaginary) and thermochemistry. We observed from this calculation that all species are found to have real positive vibrational frequencies (corresponding to stable minima) except TSs which have negative frequencies at 77i cm^{-1} (TS1), 256i cm^{-1} (TS2) and 71i cm^{-1} (TS3). Visualization of the imaginary frequencies revealed a qualitative confirmation of the existence of TSs connecting reactant- and product-like structures. IRC calculations were also performed for TS1, TS2 and TS3 at the same level of theory to investigate the connectivity of each TS with reactant- and product-like structures. IRC results show that each TS smoothly connects the reactant- and product-like structures. An IRC plot of TS2 for the main reaction is shown in Figure 3.

To understand the feasibility of the reaction path, standard reaction enthalpy ($\Delta_r H^0$) and Gibbs free energy ($\Delta_r G^0$) for the title reaction along with two other reactions were calculated (using the data provided in the supporting information, Table S18). The values of $\Delta_r H^0$ and $\Delta_r G^0$ for step 1 are found to be 26.77 and 35.75 kcal mol^{-1}, respectively, indicating that this step is endothermic at 298 K. For step 2, these values are obtained as −67.86 and −67.84 kcal mol^{-1}, respectively, which indicate the feasibility of the reaction. These values

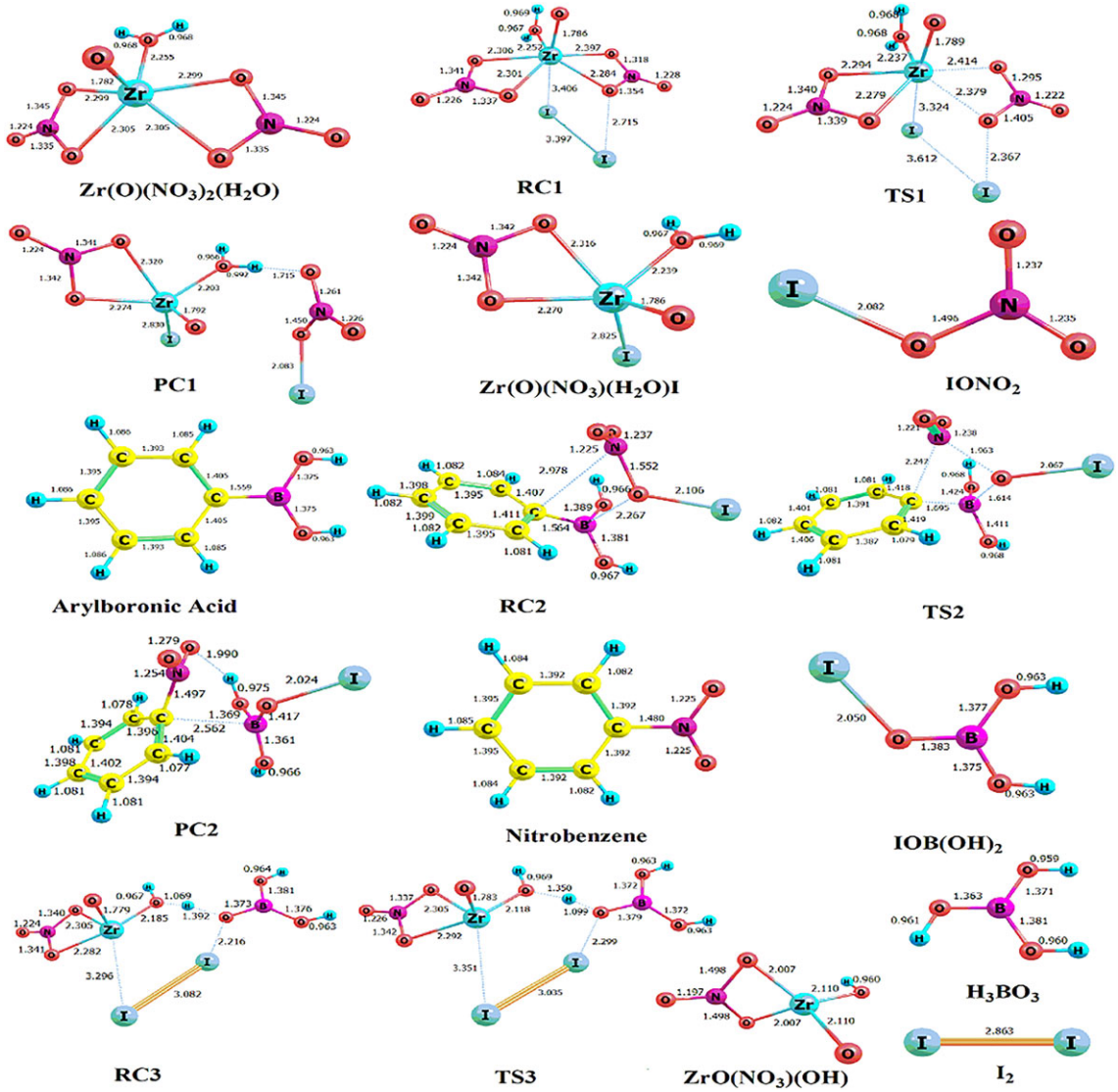

FIGURE 2 Optimized structures of species including intermediates and transition states in all steps

are found to be −25.10 and −36.64 kcal mol^{-1} for step 3 in which I_2 is regenerated. This indicates that the reaction is exothermic and feasible at room temperature and thus I_2 is easily regenerated.

Relative energies (including ZPE) for each of the species were determined (Table S18, supporting information) with respect to the reactants, setting it arbitrarily at zero, and the results are recorded in Table 3. Potential energy diagrams (Figure 4) of all steps were constructed with the results obtained at the DFT (B3LYP) level. The results show that the barrier height of step 1 is 3.57 kcal mol^{-1} and in step 2 the barrier height is 16.99 kcal mol^{-1}. Although the barrier height of TS2 is slightly higher, which is main reaction, the reaction is highly exothermic. In step 3, the barrier height is very small and equal to 1.41 kcal mol^{-1} which indicates that I_2 regenerates easily to carry out the next catalytic cycle. The involvement of each species in the mechanism is shown in Figure 5.

In conclusion, we have developed a mild, facile and efficient methodology for *ipso*-nitration of arylboronic acids catalysed by molecular iodine (10 mol%) at room temperature with moderate to excellent yields. The methodology is applicable to both aryl- and heteroarylboronic acids within a short reaction time. The new protocol is superior to the existing methodologies as it uses mild and safe nitrating source avoiding stronger acids. The most important factor is that the reaction occurs at room temperature and so is an energy-saving process. The reaction has added advantages such as it does not require any base or ligand. We have also analysed the reaction mechanism theoretically using modern DFT. Our theoretical results show that the

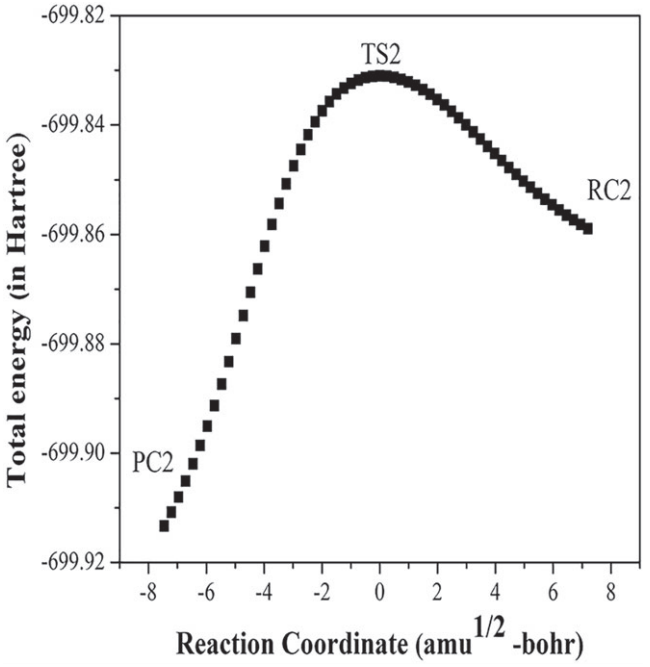

FIGURE 3 IRC plot for TS2 at B3LYP/6-311G+(d)/LanL2DZ level of theory

reaction is thermodynamically favourable which is reflected in the PES diagram (Figure 4).

2 | COMPUTATIONAL DETAILS

The geometries of all the species involved in steps 1, 2 and 3 along with intermediates (RCs and PCs) and TSs were optimized with the B3LYP functional[25,26] of DFT. During geometry optimization, the 6-311G+(d) basis set[27] was used for all elements except heavy atoms (I and Zr). Considering the strong relativistic effect of I and Zr atoms, we employed Los Alamos National Laboratory 2 double zeta (LanL2DZ) basis set with effective core potential[28] for both heavy atoms present. In order to determine the nature of stationary points on the PES, vibrational frequency calculation was made using the same level of theory at which the optimization was made. All the electronic calculations were performed using the Gaussian 09 program package.[29] The stationary points were identified to correspond to stable minima on the respective PES by ascertaining that all the harmonic vibrational frequencies were real and positive. The TSs in the reaction were obtained using synchronous transition-guided quasi-Newton method[30,31] and the first-order saddle point was characterized by the presence of only one imaginary frequency (NIMAG = 1). IRC calculations were also performed in order to ascertain that the transition of reactant to product via corresponding TS was smooth. The minimum energy path was obtained by IRC calculation.[32]

TABLE 3 Relative energies (kcal mol^{-1}) of species involved in the reaction calculated with DFT (B3LYP) and levels of theory

Reaction step	Species	Relative energy
Step 1	$Zr(O)(H_2O)(NO_3)_2 + I_2$	0.00
	RC1	28.80
	TS1	32.37
	PC1	26.33
	$Zr(O)(NO_3)(H_2O)I + IONO_2$	29.75
Step 2	$C_6H_5B(OH)_2 + IONO_2$	0.00
	RC2	73.17
	TS2	90.16
	PC2	41.16
	$C_6H_5NO_2 + IOB(OH)_2$	−67.79
Step 3	$ZrO(NO_3)(H_2O)I + IOB(OH)_2$	0.00
	RC3	−21.92
	TS3	−20.50
	$ZrO(NO_3)OH + H_3BO_3 + I_2$	−25.62

3 | EXPERIMENTAL

3.1 | General information

^1H NMR and ^{13}C NMR spectra of the products were recorded with a JNM ECS 400 MHz NMR spectrophotometer (JEOL) using tetramethylsilane as the internal standard. Chemical shift values are expressed in ppm. Coupling constants are expressed in hertz. Reactions were monitored by TLC using aluminium sheets with silica gel $60F_{254}$ (Merck). UV light and iodine vapours were used as visualizer. Chemicals were obtained from commercial sources.

3.2 | General experimental procedure for *ipso*-nitration of arylboronic acid

A 50 ml two-necked round-bottomed flask was charged with arylboronic acid (1 mmol), $ZrO(NO_3)_2{\cdot}xH_2O$ (1.5 mmol) and iodine (10 mol%) and the reaction mixture was stirred at room temperature in toluene (4 ml) under nitrogen atmosphere. After completion of the reaction (TLC), the reaction mixture was filtered with Whatman filter paper and the residue was washed with ethyl acetate followed by DCM (3 × 15 ml) and diluted with water (10 ml). The DCM extract was washed with sodium thiosulfate solution (10 ml). The separated organic layer was dried over anhydrous sodium sulfate, filtered and concentrated under reduced pressure. The crude material so obtained was purified by column chromatography on silica gel (ethyl acetate–hexane eluent). All the compounds were characterized using ^1H NMR

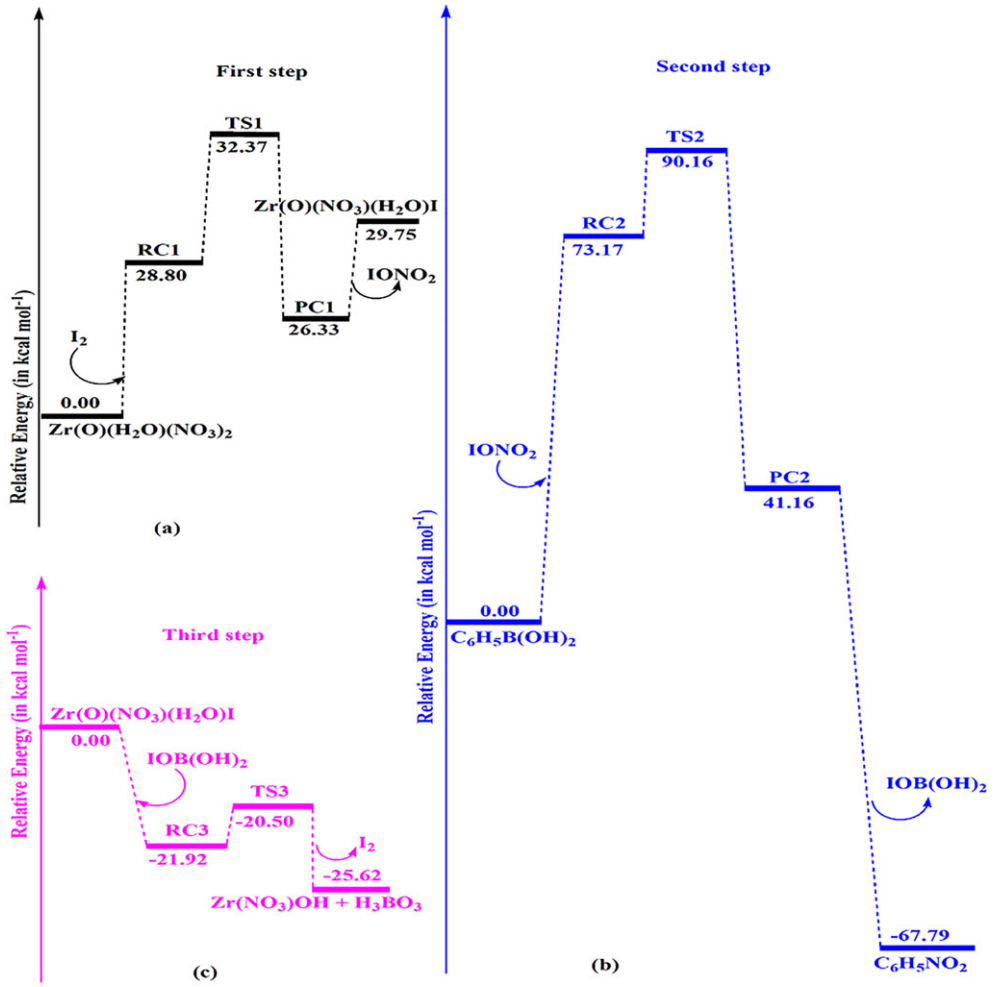

FIGURE 4 Potential energy diagrams of (a) step 1 (black), (b) step 2 (blue) and (c) step 3 (pink) at B3LYP//6-311G+(d)/LanL2DZ level of theory

and ^{13}C NMR spectroscopy and the data finally compared with those of authentic compounds.

3.3 | Characterization data of compounds

Nitrobenzene (entry 1, Table 2): Yellow liquid (109 mg, 89%); ^{1}H NMR (400 MHz, $CDCl_3$, δ, ppm): 8.21 (d, J = 8.4 Hz, 2H), 7.70–7.68 (m, 1H), 7.54 (d, J = 8 Hz, 2H); ^{13}C NMR (100 MHz, $CDCl_3$, δ, ppm): 148.2, 134.7, 129.4, 123.3.

4-Bromonitrobenzene (entry 2, Table 2): White solid (168 mg, 84%); m.p. 120–126°C; ^{1}H NMR (400 MHz, $CDCl_3$, δ, ppm): 8.08 (d, J = 7.6 Hz, 2H), 7.67 (d, J = 7.6 Hz, 2H); ^{13}C NMR (100 MHz, $CDCl_3$, δ, ppm): 147.0, 132.7, 132.5, 130.0, 125.0.

4-Formylnitrobenzene (entry 3, Table 2): White solid (128 mg, 85%); m.p. 102–106°C; ^{1}H NMR (400 MHz, $CDCl_3$, δ, ppm): 10.18 (s, 1H), 8.40 (d, J = 6.8 Hz, 2H), 8.10 (d, J = 8.4 Hz, 2H); ^{13}C NMR (100 MHz, $CDCl_3$, δ, ppm): 190.5, 151.1, 140.1, 130.6, 124.3.

3-Formylbiphenyl (entry 4, Table 2): Brown solid (119 mg, 79%); m.p. 55–60°C; ^{1}H NMR (400 MHz, $CDCl_3$, δ, ppm): 10.14 (s, 1H), 8.73–8.72 (m, 1H), 8.53–8.50 (m, 1H), 8.25 (d, J = 8 Hz, 1H), 7.81–7.77 (m, 1H); ^{13}C NMR (100 MHz, $CDCl_3$, δ, ppm): 189.9, 148.8, 137.4, 134.8, 130.5, 128.7, 124.5.

2,4-Dichloronitrobenzene (entry 5, Table 2): Yellow liquid (163 mg, 85%); ^{1}H NMR (400 MHz, $CDCl_3$, δ, ppm): 7.83 (s, 1H), 7.48–7.47 (m, 2H); ^{13}C NMR (100 MHz, $CDCl_3$, δ, ppm): 156.6, 138.7, 131.1, 130.9, 129.7, 128.8, 128.2, 127.5, 126.9, 121.0, 111.4, 55.7.

3-Chloronitrobenzene (entry 6, Table 2): White solid (135 mg, 87%); m.p. 43–50°C; ^{1}H NMR (400 MHz, $CDCl_3$, δ, ppm): 8.22–8.21 (m, 1H), 8.15–8.10 (m, 1H), 6.663–6.661 (m, 1H), 7.51–7.47 (m, 1H); ^{13}C NMR (100 MHz, $CDCl_3$, δ, ppm): 148.8, 135.5, 134.8, 128.3, 130.4, 123.9, 121.7.

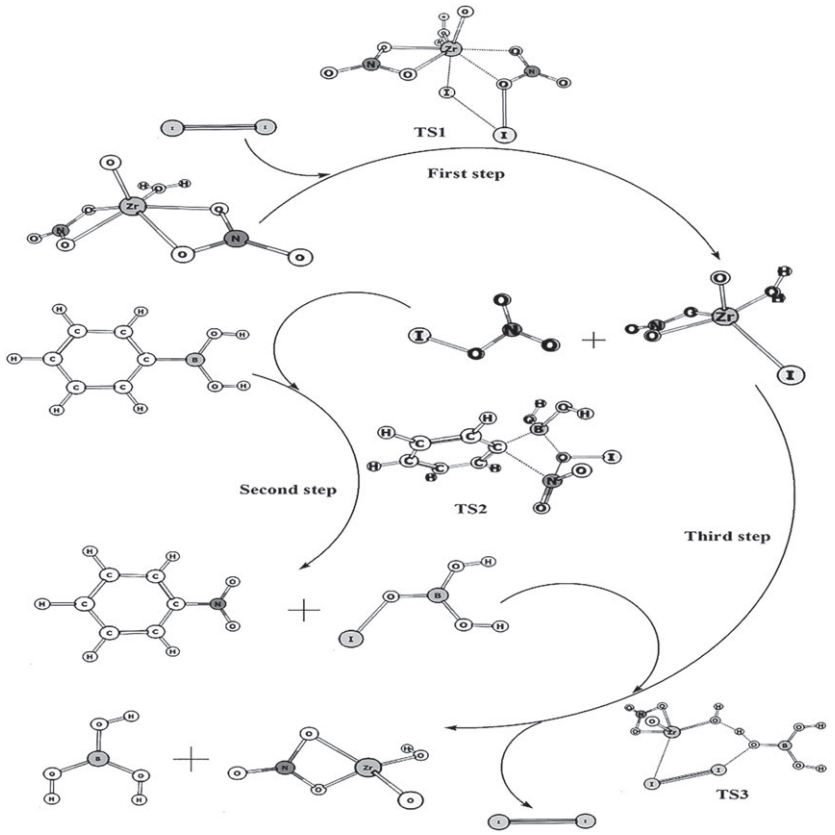

FIGURE 5 Schematic diagram of the reaction mechanism

4-Hydroxynitrobenzene (entry 7, Table 2): White solid (119 mg, 85%); m.p. 270–275°C; ^{1}H NMR (400 MHz, $CDCl_3$, δ, ppm): 8.18 (d, J = 9.2 Hz, 2H), 6.94 (d, J = 8 Hz, 2H), 6.66 (1H, br s); ^{13}C NMR (100 MHz, $CDCl_3$, δ, ppm): 161.7, 141.5, 126.4, 115.8.

4-Aminonitrobenzene (entry 8, Table 2): Yellow solid (237 mg, 89%); m.p. 330–335 C; ^{1}H NMR (400 MHz, acetone-d_6, δ, ppm): 7.95 (d, J = 6.8 Hz, 2H), 6.70 (d, J = 7.2 Hz, 2H), 6.03 (br s, 1H); ^{13}C NMR (100 MHz, $CDCl_3$, δ, ppm): 155.2, 137.3, 126.1, 112.7.

4-Methoxynitrobenzene (entry 9, Table 2): White solid (242 mg, 86%); m.p. 50–53°C; ^{1}H NMR (400 MHz, $CDCl_3$, δ, ppm): 8.22–8.19 (d, J = 9.2 Hz, 2H), 6.96 (d, J = 7.2 Hz, 2H), 3.91 (s, 3H); ^{13}C NMR (100 MHz, $CDCl_3$, δ, ppm): 164.6, 141.5, 126.0, 114.0, 56.0.

2-Methylnitrobenzene (entry 10, Table 2): Yellow liquid (107 mg, 78%); ^{1}H NMR (400 MHz, $CDCl_3$, δ, ppm): 7.13–7.09 (m, 1H), 6.75–6.73 (m, 1H), 6.65–6.62 (m, 2H), 2.29 (s, 3H); ^{13}C NMR (100 MHz, $CDCl_3$, δ, ppm): 155.5, 139.9, 129.5, 121.6, 116.1, 112.3, 21.4.

4-Methylnitrobenzene (entry 11, Table 2): White solid (110 mg, 81%); m.p. 50–55°C; ^{1}H NMR (400 MHz, $CDCl_3$, δ, ppm): 8.11 (d, J = 8.8 Hz, 2H), 7.33–7.27 (m, 2H), 2.46 (s, 3H); ^{13}C NMR (100 MHz, $CDCl_3$, δ, ppm): 146.1, 129.9, 123.5, 21.7.

2-Thiophenylnitrobenzene (entry 12, Table 2): White solid (107 mg, 83%); m.p. 40–45°C; ^{1}H NMR (400 MHz, $CDCl_3$, δ, ppm): 7.93–7.92 (m, 1H), 7.56–7.55 (m, 1H), 7.40–7.39 (m, 1H); ^{13}C NMR (100 MHz, $CDCl_3$, δ, ppm): 132.6, 128.6, 127.5, 127.0, 126.9.

3-Methoxy-2-nitropyridine (entry 13, Table 2): White solid (123 mg, 80%); m.p. 75–80°C; ^{1}H NMR (400 MHz, $CDCl_3$, δ, ppm): 8.41–8.40 (m, 1H), 8.29–8.28 (m, 1H), 7.07–7.04 (m, 1H), 4.12 (s, 3H); ^{13}C NMR (100 MHz, $CDCl_3$, δ, ppm): 156.6, 151.8, 135.1, 134.0, 116.5, 54.8.

4-Fluoronitrobenzene (entry 14, Table 2): Yellow liquid (121 mg, 86%); ^{1}H NMR (400 MHz, $CDCl_3$, δ, ppm): 8.28 (d, J = 8 Hz, 2H), 7.24 (d, J = 8 Hz, 2H), 7.39–7.36 (m, 2H); ^{13}C NMR (100 MHz, $CDCl_3$, δ, ppm): 167.6, 165.0, 144.4, 126.4, 126.3, 116.5, 116.3.

2,4-Diflouronitrobenzene (entry 15, Table 2): Yellow solid (136.74 mg, 86%); m.p. 12–15°C; ^{1}H NMR (400 MHz, $CDCl_3$, δ, ppm): 8.19–8.17 (m, 1H), 7.09–7.05 (m, 2H); ^{13}C NMR (100 MHz, $CDCl_3$, δ, ppm): 167.1, 164.4, 134.1, 128.3, 128.27, 112.2, 106.6.

2-Chloronitrobenzene (entry 16, Table 2): Yellow solid (131.88 mg, 84%); m.p. 30–33°C; ^{1}H NMR (400 MHz, $CDCl_3$, δ, ppm): 7.87–7.85 (m, 1H), 7.56–7.53 (m, 2H), 7.45–7.40 (m, 2H); ^{13}C NMR (100 MHz, $CDCl_3$, δ, ppm): 148.1, 133.2, 131.9, 127.4, 125.6.

4-Chloronitrobenzene (entry 17, Table 2): Yellow solid (138 mg, 88%); m.p. 80–85°C; ^{1}H NMR (400 MHz, $CDCl_3$, δ, ppm): 8.79 (d, J = 8.4 Hz, 2H), 7.52 (d, J = 9.2 Hz, 2H);

^{13}C NMR (100 MHz, CDCl3, δ, ppm): 146.5, 141.4, 129.6, 125.0.

NOTES

The authors declare no competing financial interest.

ACKNOWLEDGMENTS

The authors acknowledge the DST-SERB, New Delhi for financial support for this work (SERB/DST no. EMR/2016/005944). The authors are grateful to Tezpur University for the infrastructural facilities and institutional fellowship to A.M. One of the authors (N.K.G.) is grateful to UGC for DS-Kothari postdoctoral fellowship.

ORCID

Ashim Jyoti Thakur https://orcid.org/0000-0003-0923-6725
Utpal Bora https://orcid.org/0000-0002-7403-0152

REFERENCES

[1] N. Ono, *The Nitro Group in Organic Synthesis*, Wiley-VCH, Weinheim **2001**.
[2] H. Zollinger, *Color Chemistry*, Wiley-VCH, New York **1987** 161.
[3] F. R. R. Fan, Y. Yao, L. Cai, L. Cheng, J. M. Tour, A. J. Bard, *J. Am. Chem. Soc.* **2004**, *126*, 4035.
[4] M. P. Belciug, V. S. Ananthanarayanan, *J. Med. Chem.* **1994**, *37*, 4392.
[5] A. Grirrane, A. Corma, H. Garcia, *Science* **2008**, *322*, 1661.
[6] K. S. Ju, R. E. Parales, *Microbiol. Mol. Biol. Rev.* **2010**, *74*, 250.
[7] D. M. Badgujar, M. B. Talawar, S. N. Asthana, P. P. Mahulikar, *J. Sci. Ind. Res.* **2008**, *67*, 54.
[8] G. A. Olah, R. Malhotra, S. C. Narang, *Nitration: Methods and Mechanisms*, Wiley-VCH, New York **1989**.
[9] B. P. Fors, S. L. Buchwald, *J. Am. Chem. Soc.* **2009**, *131*, 12898.
[10] S. Saito, Y. Koizumi, *Tetrahedron Lett.* **2005**, *46*, 4715.
[11] V. Anuradha, P. V. Srinivas, P. Aparana, J. M. Rao, *Tetrahedron Lett.* **2006**, *47*, 4933.
[12] A. K. Bose, S. N. Ganguly, M. S. Manhas, S. Rao, J. Speck, U. Pekenely, P. Villars, *Tetrahedron Lett.* **2006**, *47*, 1885.
[13] J. F. Rustling, *Acc. Chem. Res.* **1991**, *24*, 75.
[14] M. Mandal, U. Bora, *Green Chem.* **2012**, *14*, 1873.
[15] S. Manna, S. Maity, S. Rana, S. Agasti, D. Maity, *Org. Lett.* **2012**, *14*, 1736.
[16] G. K. S. Prakash, C. Panja, T. Mathew, V. Surampudi, N. A. Petasis, G. A. Olah, *Org. Lett.* **2004**, *6*, 2205.
[17] H. Yang, Y. Li, M. Jiang, J. Wang, H. Fu, *Chem. Eur. J.* **2011**, *17*, 5652.
[18] R. R. Yadav, R. A. Vishwakarma, S. B. Bharate, *Tetrahedron Lett.* **2012**, *53*, 5958.
[19] M. Jiang, H. Yang, Y. Li, Z. Jia, H. Fu, *RSC Adv.* **2013**, *3*, 25602.
[20] X. F. Wu, J. Schranck, H. Newmann, M. Beller, *Chem. Commun.* **2011**, *47*, 12462.
[21] G. Yan, M. Yang, *Org. Biomol. Chem.* **2013**, *11*, 2554.
[22] Y. K. Liu, S. J. Lou, D. Q. Xu, Z. Y. Xu, *Chem. Eur. J.* **2012**, *16*, 13590.
[23] a)L. Zhang, Z. Liu, H. Li, G. Fang, B. D. Barry, T. A. Belay, X. Bi, Q. Liu, *Org. Lett.* **2011**, *13*, 6536. b)S. Das, R. Borah, R. R. Devi, A. J. Thakur, *Synlett* **2008**, *18*, 2741. c)M. N. Ren, C. Cai, R. S. Yang, *RSC Adv.* **2013**, *3*, 7182.
[24] S. S. Shinde, M. S. Said, T. B. Surwase, P. Kumar, *Tetrahedron Lett.* **2015**, *56*, 5916.
[25] K. Kim, K. D. Jordan, *J. Phys. Chem.* **1994**, *98*, 10089.
[26] P. J. Stephens, F. J. Devlin, C. F. Chabalowski, M. J. Frisch, *J. Phys. Chem.* **1994**, *98*, 11623.

SUPPORTING INFORMATION

Additional supporting information may be found online in the Supporting Information section at the end of the article.

How to cite this article: Mahanta A, Gour NK, Sarma PJ, et al. A convenient room temperature *ipso*-nitration of arylboronic acid catalysed by molecular iodine using zirconium oxynitrate as nitrating species: An experimental and theoretical investigation. *Appl Organometal Chem*. 2019;e4951. https://doi.org/10.1002/aoc.4951